



Evolutional Based Optimization Analysis for Three-element Control System

I. M. Chew¹, Filbert H. Juwono² and W. K. Wong³

^{1,3}Department of Electrical and Computer Engineering, Curtin University Malaysia, Miri, Sarawak Malaysia

²Department of Electrical and Electronic Engineering, Xi'an Jiaotong-Liverpool University, China

Received 19 May 2023, Revised 30 Jan. 2024, Accepted 21 Feb. 2024, Published 1 Mar. 2024

Abstract: This paper presents a multi-objective optimization analysis to improve the controller tuning of three-element control loop for the best fit to both its servo and regulatory control objectives during the process operations. The existing Proportional-Integral-Derivative (PID) controller tuning for the three-element control loop is challenging because the best setting of each controller is obtained during the concurrent analysis, but all controller settings affect the control performance of other control loops and the output responses. Furthermore, this paper highlights the determination of Upper Limit (UL) and Lower Limit (LL) bounds by using the necessity criterion of Routh-Hurwitz stability analysis. The Genetic Algorithm (GA) and Particle Swarm Optimization (PSO) are used as the optimization algorithms to improve the control performances. Both optimization analysis are operated by using a developed Graphical User Interface (GUI) via MATLAB software. At the same time, the optimized PID controller settings are applied to the steam boiler drum function of the LOOP-PRO simulator. Both GA and PSO outperform the manual tuning for the three-element loop. Among them, GA performs better than PSO even though both methods are capable of suggesting highly satisfactory performances.

Keywords: Multiple loop, Upper and lower bounds, Multi-objective optimization, Graphical user interface, Curve and indexes performances

1. INTRODUCTION

Nowadays, industrial processes have commonly applied the Proportional-Integral-Derivative (PID) controller tuning [1] in closed control loops, where the servo and regulatory objectives are considered. It has been reported that the existing PID controller tuning methods, such as Ziegler-Nichols (ZN) and Internal Model Control (IMC), are adequate to control single-loop system. In particular, IMC applies different formulas for the respective servo and regulatory controls. The main problem is that the applied PID controller of each control loop will affect or deteriorate the control performance of the other control loops [2], [3]. Besides, both the aforementioned tuning methods rely on complex mathematical calculations and engineers' experiences in doing the refined tunings [4]. Therefore, two questions arise. How could the engineers obtain the optimized tuning of three-element loops without involving complex mathematical calculation? How to obtain the best tuning for reasonable performances of all interacted control loops? We recommend a multi-objective optimization analysis such as Genetic Algorithm (GA) and Particle Swarm Optimisation (PSO) as one alternative approach to improve the existing PID controller tunings. The GA optimization algorithm is motivated by the biological mechanism of natural selection, where the harsher individual is likely

to be the winner of a competitive world. The operation is started from an initial population that comprises some chromosomes and each one of them will correlate to a result of the given problem [5]. The application of operators to form new children through crossover and mutation possibly are more excellent than their parents. The best solution of the new chromosome is determined by the algorithm of the fitness function. Iteration repeats many times to improve the new best chromosomes until it meets the set iteration in the fitness function. Ultimately, the chromosome with the most fixed fitness degree is chosen as the most compatible solution for the optimization analysis.

PSO refers to the social behaviour of nature's elements for instance birds flocking or fish schooling [6]. PSO algorithm works on regular selection of the fittest child to survive after many iterations. Initially, a set of particles known as the population is randomly selected. These particles with respective velocities and positions are evaluated with predetermined fitness values to obtain the personal and global best values. Personal best reflects the best individual particle composition, while global best represents the goal position of all particles [7].

This paper primarily aims at improving the performance



of the three-element loop function via multi-objective optimization analysis, where the results are comparatively discussed with the existing manually tuning techniques. The introduction and problem are highlighted at the beginning of this paper. Section 2 presents the literature review and previous works of the three-element control loop, GA and PSO. Section 3 highlights the logical flow of the research, which includes the formulation of stability margin for the primary loop, secondary loop and feedforward algorithm. This is followed by the multi-objective optimization algorithm to produce the best controller tuning, which has been determined by Integral Error measurement. Section 4 describes the analysis and results via a case study on the three-element steam drum function. The multi-objective optimization analysis is then validated by the three-element steam drum control function of the LOOP-PRO simulator. In addition, a Graphical User Interface (GUI) is developed to allow multi-objective function to operate in a consistent environment that could visualize the optimization result. Finally, Section 5 concludes the research findings and proposes future improvements to the multi-objective optimization analysis.

2. LITERATURE REVIEW

PID-based tuning approaches have been used in many applications for improving overall control performance. MATLAB/Simulink has been used to develop application that communicates the boiler with the PID control [2]. The author of paper [8] modified the fractional order relay based automatic tuning of PI^λD controller for stable processes with load disturbance via adjusting the phase margin, λ .

In order to cope with unpredictability in the outlet parameters, the authors in [9] used an optimization approach to forecast the changes for the inlets for PID control at the same levels. Whereas, the paper [10] worked on the different interacted loop levels. The authors of the paper [11] compared tracking accuracy and disturbance rejection ability in various iterative learning controls, which were adopted with feedforward function. The authors of the paper [12] compared several control systems for decreasing parameter deviations of both servo and regulatory controllers by using feedforward and feedback loops. The paper [13] proposed a robust-based \mathcal{H}_∞ state feedback controller to an industrial boiler and then examined its stability and performance via Linear Matrix Inequalities (LMIs) techniques. The authors of the paper [14] applied Proportional-Integral (PI)-based feedforward and feedback control to a piezoelectric actuated micro positioning stage. Furthermore, the paper [15] applied a feedforward strategy to counter the impact of disturbance for a lab-scale three series flotation tank system.

GA refers to direct analogy, such as natural evolution, to perform optimization that solves complex engineering problems. GA has been used in many applications. The authors of paper [16] used GA to align controller parameters when the disturbances were presented. The paper [17] applied the linear quadratic Gaussian controller operated by

GA, to reduce the frequency divergences and settling time in the load frequency control. The paper [18] applied the GA algorithm to reduce the computational cost during the optimization analysis. In addition, the authors of paper [19] comparatively studied the response surface methodology and GA for optimizing the laser welding process. The paper [20] applied GA optimization to produce the shortest rising time of PID-based cruise control system, whereas [21] adjusted mutation operators to solve Max One problem and compared it with the result from conventional GA usage. Besides, the authors of the paper [22] applied optimization to regulate the receiver's mass flow rate, thereby minimizing the solar energy fluctuation.

PSO applies the social-psychological theory of animals, which is adapted to various research studies. The authors of paper [23] minimized power losses of the distribution system, which is installed with a shunt compensator by using PSO optimization. The paper [24] designed a feedforward controller to expel inconsistent hysteresis behaviours of a piezoelectric stack actuator-driven system. In addition, the paper [25] tuned PI parameters of the boiler turbine unit with hybrid PSO, whereas the authors of paper [26] solved H_∞ optimization problem of a novel three-element-type DVA model with a grounded negative stiffness spring by combining a traditional theory and an intelligent algorithm. In the paper [6], the authors discussed the optimization approaches of the swarm intelligence strategy. Besides, the paper [27] designed the optimized fuel composition and the paper [28] applied optimization to obtain the best controller tuning in the controlled loops.

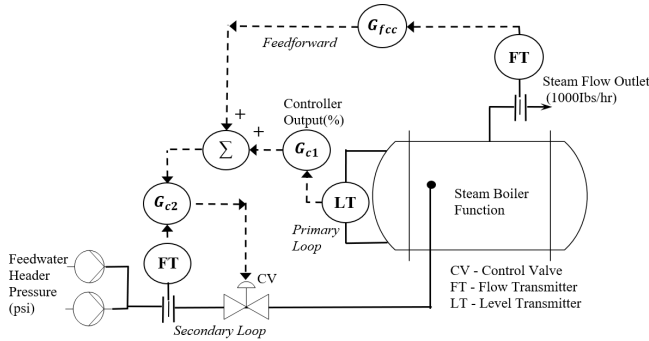
It is observable that the applied PID control strategies have solely focused on either one of the servo or regulatory control objectives. In fact, both control objectives are essential in the control operations. Thereby, it is resolutely proposing to generate the most compatible controller settings best fixed to both servo and regulatory controls using optimization analysis. Moreover, this paper recommends determine the bound settings of the analyzed parameters for reducing the computational cost.

3. STABILITY AND PERFORMANCE ANALYSIS OF THREE-ELEMENT CONTROL LOOP

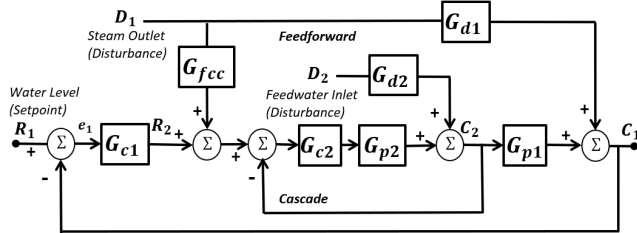
A. Stability Margin of Three-element Control Loop

The optimization analysis takes account of the parameter settings to the applied algorithms that correspond to the reduced iterations and improved best solutions [9]. Two of the essential parameter settings are the Upper Limit (UL) and Lower Limit (LL) settings, which are applicable to the three-element loop. Note that a three-element loop comprises the feedforward plus cascade control algorithms. The cascade control algorithm comprises secondary and primary loops. All the setpoint and disturbances are presented in the form of First Order plus Dead Time (FOPDT) models. In this research, steam boiler drum function of the LOOP-PRO simulator is set to operate in three-element loop. The secondary loop is a self-regulating configuration

of flow control, whereas the primary loop is an integrating configuration of level control. Fig. 1 (a) shows both flow and level controls of a steam boiler drum function, whereas Fig. 1 (b) shows the block diagram of the three-element loop.



(a) Three-element based Steam Boiler Drum Function



(b) Block Diagram of Three-element Loop

Figure 1. Three-element Loop of Steam Drum Boiler Function for the Water Level Control

1) Analysis of the cascade control algorithm

Analysis of the cascade loop comprises the primary and secondary loops [3]. The self-regulating FOPDT transfer function (G_{p2}) is presented by (1)

$$G_{p2} = \frac{K_{p2}e^{-\theta_{p2}s}}{\tau_{p2}s + 1}, \quad (1)$$

where, K_{p2} is the process gain (secondary loop), τ_{p2} is the process time constant (secondary loop), and θ_{p2} is the process dead time (secondary loop). Approximating the exponential term by using Taylor Series approximation, $e^{-\theta_{p2}s} \approx 1 - \theta_{p2}s$ yields (2)

$$G_{p2} = \frac{K_{p2}(1 - \theta_{p2}s)}{\tau_{p2}s + 1} = 0. \quad (2)$$

The secondary loop PI controller algorithm (G_{c2}) is illustrated by (3)

$$G_{c2} = \frac{K_{c2}s + K_{i2}}{s}, \quad (3)$$

where K_{c2} is the proportional gain (secondary loop) and K_{i2}

is the integral gain (secondary loop). Incorporating both G_{p2} and G_{c2} into the closed-loop transfer function (see [28]), the denominator of the secondary loop transfer function is given by (4).

The stability analysis is determined by the necessity condition of the Routh-Hurwitz stability. Arranging parameter values in sequential order gives (5)

$$(\tau_{p2} - K_{p2}K_{c2}\theta_{p2})s^2 + (1 + K_{p2}[K_{c2} - K_{c2}\theta_{p2} + K_{i2}]) = 0 \quad (5)$$

All the parameters of the polynomial equation should have the same polarities, assuming all parameters to have the final value > 0 . From the terms s^2 , $\tau_{p2} - K_{p2}K_{c2}\theta_{p2} > 0$, arranged in K_{c2} term gives (6) as the UL.

$$K_{c2} < \frac{\tau_{p2}}{K_{p2}\theta_{p2}}. \quad (6)$$

From the term s , $1 + K_{p2}K_{c2} - K_{p2}K_{i2}\theta_{p2} > 0$, arranged in K_{i2} term, and using $K_{i2} < \frac{1+K_{p2}K_{c2}}{K_{p2}\theta_{p2}}$ and $K_{i2} = \frac{K_{c2}}{\tau_{i2}}$, we obtain (7) as the LL.

$$\tau_{i2} > \frac{K_{c2}K_{p2}\theta_{p2}}{1 + K_{p2}K_{c2}}. \quad (7)$$

Therefore, the bound settings for K_{c2} and τ_{i2} are identified. The secondary closed-loop function (CL_2) is nested into the primary loop as depicted in Fig. 2.

The integrating FOPDT model of the primary loop (G_{p1}) is given by (8)

$$G_{p1} = \frac{K_{p1}e^{-\theta_{p1}s}}{s}, \quad (8)$$

where K_{p1} is the process gain (primary loop) and θ_{p1} is the process dead time (primary loop). Approximate the (8) using Pade Approximation gives $e^{-\theta_{p1}s} \approx (1 - 0.5\theta_{p1}s)/(1 + 0.5\theta_{p1}s)$, which yields (9)

$$G_{p1} = \frac{K_{p1}(1 - 0.5\theta_{p1}s)}{s(1 + 0.5\theta_{p1}s)}. \quad (9)$$

The PI controller model for primary loop (G_{c1}) is given by (10)

$$G_{c1} = \frac{K_{c1}s + K_{i1}}{s}, \quad (10)$$

where K_{c1} is the proportional gain (primary loop) and K_{i1} is the integral gain (primary loop). Incorporating CL_2 into the closed-loop function of the primary loop yields a new transfer function as (11)

$$\frac{C_1}{R_1} = \frac{G_{p1}CL_2G_{c1}}{1 + G_{p1}CL_2G_{c1}}. \quad (11)$$

From (11), we can get (12)

$$\frac{C_1}{R_1} = \frac{G_{p1}G_{p2}G_{c1}G_{c2}}{1 + G_{p2}G_{c2} + G_{p1}G_{p2}G_{c1}G_{c2}}. \quad (12)$$

$$\frac{G_2}{R_2} = \frac{(K_{p2}K_{c2} - K_{i2}K_{p2}\theta_{p2})s - (K_{p2}K_{c2}\theta_{p2}s^2) + K_{p2}K_{i2}}{(\tau_{p2}s^2 + s) + (-K_{p2}K_{c2}\theta_{p2}s^2 + (K_{p2}K_{c2} - K_{p2}K_{i2}\theta_{p2})s + K_{p2}K_{i2})}. \quad (4)$$

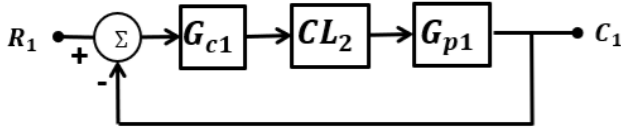


Figure 2. The Secondary Closed Loop is nested in the Primary Loop

Applying the necessity condition of the Routh-Hurwitz criterion, all the polynomial parameters should have the same polarity. The denominator part of (12) is re-defined as $1 + G_{p2}G_{c2} + G_{p1}G_{p2}G_{c1}G_{c2} = 0$ to form (13).

Arranging all the variables based on the order of terms and representing the expression polynomial parameters with alphabets give $(\mathbf{a})s^5 + (K_{c1}\mathbf{e} + \mathbf{b})s^4 + (K_{i1}\mathbf{e} + K_{c1}\mathbf{f} + \mathbf{c})s^3 + (\mathbf{d} + K_{c1}\mathbf{g} + K_{i1}\mathbf{f})s^2 + (K_{c1}\mathbf{h}K_{i1}\mathbf{g})s + K_{i1}\mathbf{h} = 0$, where $\mathbf{a} = 0.5\theta_{p1}(\tau_{p2} - K_{p2}K_{c2}\theta_{p2})$, $\mathbf{b} = (\tau_{p2} - K_{p2}K_{c2}\theta_{p2}) + 0.5\theta_{p1}(1 + K_{p2}K_{c2} - K_{p2}K_{i2}\theta_{p2})$, $\mathbf{c} = (1 + K_{p2}K_{c2} - K_{p2}K_{i2}\theta_{p2}) + 0.5\theta_{p1}K_{p1}K_{i2}$, $\mathbf{d} = K_{p2}K_{i2}$, $\mathbf{e} = 0.5K_{p1}K_{p2}K_{c2}\theta_{p1}\theta_{p2}$, $\mathbf{f} = -K_{p1}K_{p2}K_{c2}\theta_{p2} - 0.5K_{p1}K_{p2}\theta_{p1}(K_{c2} - K_{i2}\theta_{p2})$, $\mathbf{g} = K_{p1}K_{p2}(K_{c2} - K_{i2}\theta_{p2}) - 0.5\theta_{p1}K_{p1}K_{p2}K_{i2}$, and $\mathbf{h} = K_{p1}K_{p2}K_{i2}$.

Regarding the coefficient of term s^3 , after we substitute the $(K_{i1}\mathbf{e} + K_{c1}\mathbf{f} + \mathbf{c})$ with its terms and rearrange the formula into the terms of K_{c1} , it becomes $[1 + K_{p2}(K_{c2} - K_{i2}\theta_{p2}) + 0.5K_{p1}\theta_{p1}K_{i2}] + K_{c1}(-K_{p1}K_{p2}K_{c2}\theta_{p2} - 0.5\theta_{p1}K_{p1}K_{p2}(K_{c2} - K_{i2}\theta_{p2})) + 0.5K_{i1}K_{p2}K_{c2}\theta_{p1}\theta_{p2} > 0$. Re-arranging the component into the term of K_{c1} and expecting all parameters to have the final value > 0 , the UL can be rewritten as (14).

Besides, the order of terms s^0 is referred as LL that gives (15)

$$K_{i1} > 0. \quad (15)$$

As $K_{i1} > 0$, we also know that $\tau_{i1} > 0$. As $\tau_{i1} > 0$, any value of τ_{i1} greater than 0 is substantial to maintain stability for the closed-loop process.

On the other hand, the feedforward control algorithm could be described and analyzed as follows. The feedforward algorithm is purposely used to optimize the regulation of the inlet in a fast responding to the load changes of the outlet [3]. From Fig. 1 (b), the feedforward algorithm of closed-loop (G_{ffc}) notes the change of the steam outlet at the output and instantly adjusts the weight of the inlet water at the input to alleviate the impact of load changes to the regulated water level of the steam drum boiler function. As it is an integrating process, the FOPDT model of the feedforward function (G_{d1}) is given by (16)

$$G_{d1} = \frac{K_{d1}e^{-\theta_{d1}s}}{s}, \quad (16)$$

where K_{d1} is the disturbance gain and θ_{d1} is the disturbance dead time. The function of primary loop in Fig. 1 (b) is given by (17)

$$C_1 = G_{d1}D_1 + G_{p1}(D_1G_{ffc} + CL_2C_{c1}e_1). \quad (17)$$

The expression of e_1 is expressed by (18)

$$e_1 = (R_1 - C_1). \quad (18)$$

Substituting (17) into (18) and arranging the terms give (19)

$$C_1(1 + G_{p1}C_{c1}) = \frac{G_{d1}D_1}{CL_2} + G_{p1}G_{ffc}D_1 + G_{p1}G_{c1}R_1. \quad (19)$$

The feedforward algorithm does not sabotage the closed-loop stability, even this algorithm has limitations to eliminate the steady-state offset. Ultimately, the regulatory control model is given by (20)

$$\frac{C_1}{D_1} = \frac{G_{d1} + G_{p1}CL_2G_{ffc}}{1 + G_{c1}G_{p1}CL_2}, \quad (20)$$

where G_{ffc} is the control algorithm of the feedforward function. For the numerator part, we anticipate the ‘‘excellent’’ control whereby the controlled variable abides at the setpoint regardless of deviation at the load variable, D_1 . Therefore, the set value remains unchanged ($R(s) = 0$), and we anticipate $C_1(s) = 0$, although $D(s) \neq 0$, and (20) is given by $G_{d1} + G_{p1}CL_2G_{ffc} = 0$.

The secondary loop responses faster than the primary loop. Therefore, its response can be ignored when determining the G_{ffc} , which gives the ideal feedforward algorithm given by (21)

$$G_{ffc} = -\frac{G_{d1}}{G_{p1}}. \quad (21)$$

The process model gain is primarily affecting the output. Therefore, a static feedforward algorithm can be developed, in which to only cover the ratio of K_d to the K_{p1} . Besides, the feedforward ratio (Γ) is applied for the optimization analysis that allows obtaining the better ratio value of inverse relation for K_d to the K_{p1} . Therefore, the feedforward control algorithm with ratio, G_{ff} , is given by (22)

$$G_{ff} = -\Gamma \frac{K_d}{K_{p1}}. \quad (22)$$

The tuning ratio, $\Gamma \in (0, 2)$ is the used scalar parameter to tune the best gain of regulatory control. In conventional tuning, Γ is tuned based on trial and error, but in computational optimization analysis, this factor is computationally analyzed together with the PI controllers.

$$1 + \frac{K_{p1}(1 - 0.5\theta_{p1}s)}{s(1 + 0.5\theta_{p1}s)} * \frac{(K_{p2}K_{c2} - K_{i2}K_{p2}\theta_{p2})s - K_{p2}K_{c2}\theta_{p2}s^2 + K_{p2}K_{i2}}{(\tau_{p2} - K_{p2}K_{c2}\theta_{p2})s^2 + (1 + K_{p2}K_{c2} - K_{p2}K_{i2}\theta_{p2})s + K_{p2}K_{i2}} * \frac{K_{c1}s + K_{i1}}{s} = 0 \quad (13)$$

$$K_{c1} < \frac{[1 + K_{p2}(K_{c2} - K_{i2}\theta_{p2}) + 0.5K_{p1}\theta_{p1}K_{i2}] + 0.5K_{p1}K_{i1}K_{p2}K_{c2}\theta_{p1}\theta_{p2}}{K_{c1}(K_{p1}K_{p2}K_{c2}\theta_{p2} + 0.5K_{p1}\theta_{p2} + 0.5K_{p1}K_{p2}\theta_{p1}(K_{c2} - K_{i2}\theta_{p2}))} \quad (14)$$

2) *Formulation of Multi-Objective Based Optimization Algorithm and Optimization Parameters Setting*

For the optimization analysis, the design problems include: $K_{c2} = x(1)$; $K_{i2} = x(2)$; $K_{c1} = x(3)$; $K_{i1} = x(4)$; $\Gamma = x(5)$. Replacing the selected design variables in (3), (10), and (22) respectively, the redefined controller algorithms for optimization could be written as (23) - (25).

Secondary loop PI controller:

$$G_{c2} = \frac{x(1)s + x(2)}{s}, \quad (23)$$

Primary loop PI controller:

$$G_{c1} = \frac{x(3)s + x(4)}{s}, \quad (24)$$

Feedforward algorithm:

$$G_{ff} = -x(5) \frac{K_{d1}}{K_{p1}}, \quad (25)$$

The error is the accumulative net area of the response when servo and regulatory controls are parallel conducted and evaluated by the algorithm. Overall, error measurements for servo and regulatory controls are shown in (26) - (27) and incorporated to give (28).

Error 1 (servo control):

$$e_1 = 1 - \text{step} \left(\frac{C_1}{R_1} \right), \quad (26)$$

Error 2 (regulatory control):

$$e_2 = 1 + \text{step} \left(\frac{C_1}{D_1} \right), \quad (27)$$

The total integral error:

$$J = \min_e f(x) = \int abs(e_1) dt + \int abs(e_2) dt, \quad (28)$$

where $\text{step}(\cdot)$ denotes transfer functions for the process or disturbance and $\text{abs}(\cdot)$ denotes absolute function.

Source coding of the objective function and optimization analysis are formulated based on the multi-objective optimization analysis flowchart of Fig. 3. All the source coding are adapted to a developed Graphical User Interface (GUI), supported by MATLAB simulation tool, which would be demonstrated in the next section. Equations (6), (7), (14), and (15) are respectively used for determining bound settings at the GUI. Nonetheless, few parameter settings still

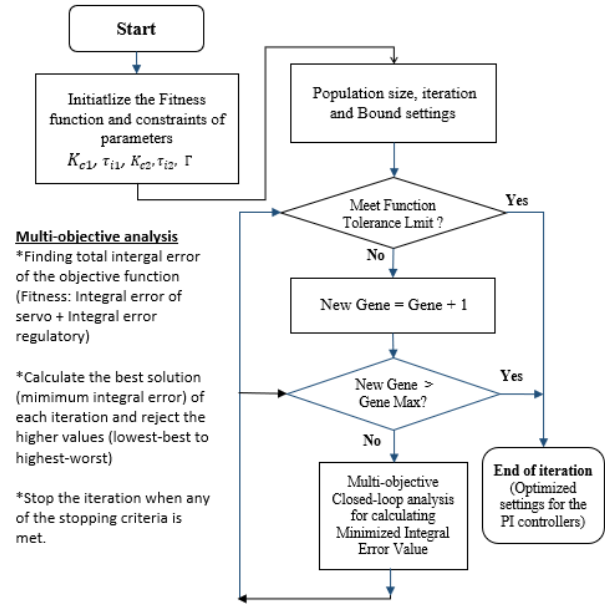


Figure 3. Flowchart of Multi-objective Optimization Analysis

apply default settings in the optimization algorithm, which consists of maximum iteration of 100 and population size of 20. Additionally, the mutation rate for GA and damping ratio for PSO are fairly set to 0.8.

3) *Integral Error Measurement*

The performance indexes of all control loops set by various control methodologies are quantitatively measured by using integral error measurement. As noted, the integral error is obtained by measuring the total area deviation under the curve of process variables versus the setpoint condition. The smaller the deviated net area, the less integral area value and the higher controllability to the process loops.

The produced errors are cumulatively measured by Integral Absolute Error (IAE), Integral Square of Error (ISE), and Integral over Time for Absolute Error (ITAE) during the simulation analysis. IAE unites the entire error value in the cycles over the period. ITAE multiplies the entire error over the period and then incorporates the sum error unit. ISE integrates the square of the entire error over period that enlarges small errors when comparing the performance of several control loops. All the integral errors are simulated by MATLAB software. Besides, the IAE is applied to

both GA and PSO multi-objective optimization analysis for calculating the most optimum controller values that produce the least integral error values.

4. ANALYSIS AND RESULT DISCUSSION

A. The Identified Models from the LOOP-PRO Simulator

This research applies the identified process models of the single, cascade, and three-element loop steam boiler function of the LOOP-PRO simulator. All the identified models are in the FOPDT terms as tabulated in Table I.

While operating the steam boiler drum function of the Loop-PRO simulator, set the function to a single-loop activate one process model to control the water level. Setting the function to the cascade loop utilizes a self-regulated flow control loop as the secondary loop, and is embedded into the primary loop to control the water level of steam drum function. Therefore, there are two identified process models. The terms of FOPDT models for primary and secondary loops are referring to (1) and (8). Furthermore, the three-element control loop applies the Γ to measure the regulated water inlet, which can be referred to (22) and it involves another disturbance model at the steam outlet.

B. Description of the Obtained Bound Limits for Optimization

The bound settings for both primary and secondary loop controllers help in narrowing down the specific searching region, therefore, reducing the analysis period and computational costs for the optimization analysis.

For the secondary loop's limit, see Table I and substitute $K_{p2} = 0.268$, $\tau_{p2} = 0.257$ and $\theta_{p2} = 0.114$ into (6) and (7) to get the limit settings of $0 < K_{c2} < 8.75$ and $\tau_{i2} > 0.1$. We can set unit number for τ_{i2} so optimization analysis will analyses corresponding value of K_{c2} in the optimization analysis.

For the primary loop's limit, see Table I and substitute $K_{p2} = 0.268$, $\tau_{p2} = 0.257$, $\theta_{p2} = 0.114$, $K_{p1} = 0.037$, and $\theta_{p1} = 0.944$ to calculate (15), which will result on $0 < K_{c1} < 62.6$. As τ_{i1} is greater than 0, any positive τ_{i1} values are acceptable for optimizing corresponding K_{c1} value.

C. Three-element Optimization Toolbox for the Genetic Algorithm and Particle Swarm Optimization

Analysis of the three-element loop covers feedforward and cascade control algorithms that were incorporated into a developed GUI toolbox, that is operated by MATLAB software. Three-element GUI toolbox for both both GA and PSO optimization with other parameter settings are illustrated in Fig. 4.

The GUI toolbox's operation is started by keying in the process model parameters, UL and LL bounds. The optimization analysis type is selected between GA or PSO. Then, click the "RUN" button to start the optimization analysis. Once the optimization analysis is completed, the optimized PI controller settings for primary and secondary

loops are displayed in the respective columns at the right bottom of the GUI screen. Besides, the response curves for both servo and regulatory controls are revealed in the figure columns, which reflect that the recommended PI controller tunings have given the decayed response in the three-element control loop.

D. Controller Settings

PI controller tuning for all methods are illustrated in Table II. For the manual tuning, all the single, cascade and three-element (manual tuning) were calculated by using IMC tuning method. The single loop has only have one unit PI controller setting, whereas, the cascade loop has two PI controller settings. Moreover, the three-element control loop has accounted Γ as another additional composition of the tuning factor. On the other hand, PI controllers for both three-element GA and PSO were obtained by operating the simulation analysis supported by Three-element GUI Toolbox, which has been described in previous section.

E. Description of the Performance Indexes

Fig. 5 shows the performance indexes or integral error measurements in the SIMULINK environment of the MATLAB software. For the single loop, we develop a similar diagram by ignoring the secondary loop and feedforward function. For the cascade loop, we develop a similar diagram but excluded the feedforward function. For the three-element control loop, we develop an exactly similar diagram of this figure to measure the integral errors. The obtained performance indexes for PI controller tuning of all control loops are tabulated in Table III, where the relative performance indexes of IAE, ISE, and ITAE are mainly compared between three-element loops with the non-three-element loops.

As noted in the previous section, the smaller deviated net area gives lesser integral error values, which means a stronger tendency of process variables to abide by the setpoint in a shortened period. Therefore, the better performance of the control system. IAE measures absolute error of area, ISE measures large overshoots and ITAE measures consistency of control performance within a period. In comparing single and cascade loops, this is found that the single loop has performed better for the setpoint condition as it has lower integral errors (IAE and ISE). Three-element (manual tuning) is applied to further improve outlet and inlet disturbances with lower outlet and inlet disturbances (for all IAE, ISE and ITAE), nevertheless still has degraded setpoint due to the complexity of the control loops. In optimizing the control loops, the GA and PSO are applied. The applied Γ (refer to (22)) in the multi-objective optimization analysis recommended the proper settings for improving the control of disturbances. Total IAE, ISE and ITAE values for all three-element loops are calculated (recorded to Table III, column 6 onwards). Ultimately, the total IAE, ISE and ITAE among three-element are compared and explained.

GA achieved improvements on 13% for IAE, 11.38% for ISE and 16.84% for ITAE measurements. Whereas,

TABLE I. Single, Cascade and Three-element Control Loop Models

| Control Loop | Secondary Loop Model | Primary Loop Model | Outlet Disturbance Model |
|--------------------|-------------------------------------|------------------------------|-------------------------------|
| Single Loop | N/A | $\frac{0.036e^{-1.002s}}{s}$ | N/A |
| Cascade Loop | $\frac{0.268e^{-0.114s}}{0.257s+1}$ | $\frac{0.037e^{-0.944s}}{s}$ | N/A |
| Three-element Loop | $\frac{0.268e^{-0.114s}}{0.257s+1}$ | $\frac{0.037e^{-0.944s}}{s}$ | $\frac{-0.137e^{-0.615s}}{s}$ |

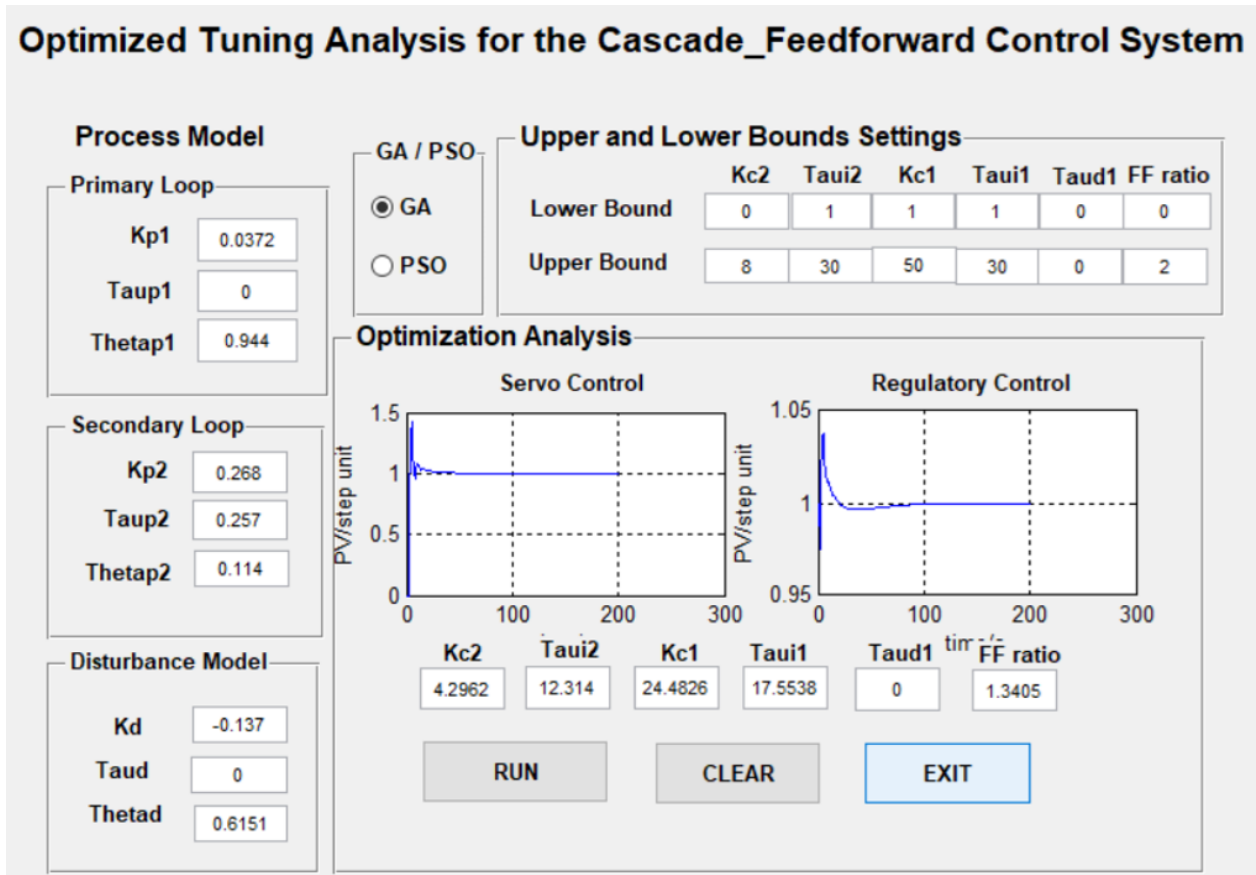


Figure 4. Three-element Optimization GUI Toolbox

TABLE II. Proportional-Integral Parameters Tuning for Single, Cascade and Three-element Control Loops

| Control Tunings | Secondary Loop | | Primary Loop | | ratio |
|-----------------------------------|----------------|----------------|--------------|----------------|----------|
| | $K_{c2}, \%$ | τ_{i2}, s | $K_{c1}, \%$ | τ_{i2}, s | Γ |
| Single Loop | - | - | 11.6 | 7.34 | 0 |
| Cascade Loop | 8.09 | 3.54 | 6.54 | 9.02 | 0 |
| Three-element (manual tuning) | 4.27 | 8.2 | 13.67 | 8.16 | 1 |
| Three-element with Γ (PSO) | 1.83 | 7.61 | 27.53 | 10.65 | 1.091 |
| Three-element with Γ (GA) | 4.17 | 6.76 | 13.77 | 8.574 | 1.263 |

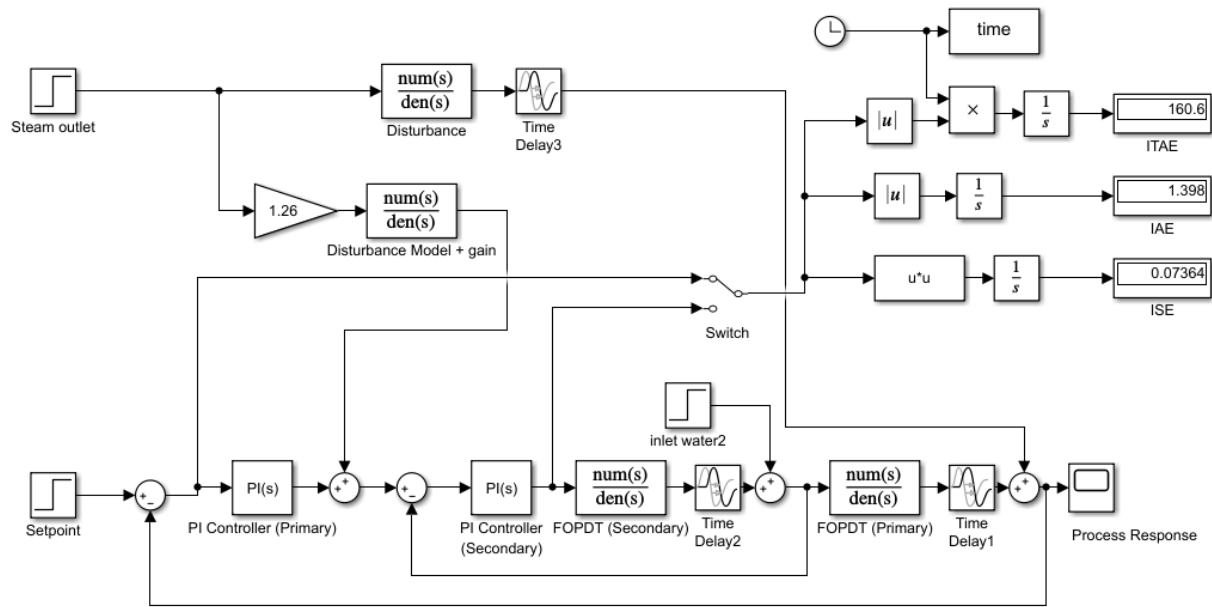


Figure 5. Simulink Diagram for the Integral Error Measurement of Three-element loop

TABLE III. The Integral Error Measurement and the Percentage Improvements of the Optimization Analysis

| Control Loop | Setpoint (Water Level) | | | Outlet Dist. (Steam) | | | Inlet Dist. (Feedwater) | | |
|---|------------------------|-------|-------|----------------------|-------|-------|-------------------------|-------|-------|
| | IAE | ISE | ITAE | IAE | ISE | ITAE | IAE | ISE | ITAE |
| Single Loop | 4.286 | 2.15 | 65.3 | 2.382 | 0.468 | 40.38 | 4.28 | 2.51 | 65.32 |
| Cascade Loop | 8.55 | 4.06 | 177.5 | 2.37 | 0.223 | 58.76 | 4.278 | 1.476 | 77.07 |
| Three-element (manual tuning) | 6.803 | 3.316 | 124.7 | 1.648 | 0.111 | 39.4 | 2.37 | 0.38 | 55.44 |
| Three-element with Γ (PSO) | 5.99 | 3.09 | 101.7 | 2.022 | 0.184 | 46.34 | 3.313 | 0.795 | 63.32 |
| Three-element with Γ (GA) | 5.955 | 2.967 | 101.9 | 1.397 | 0.07 | 34.84 | 2.64 | 0.599 | 48.53 |
| Manual tunings (Setpoint + outlet disturbance) | Total IAE | | | Total ISE | | | Total ITAE | | |
| | 8.451 | | | 3.427 | | | 164.1 | | |
| GA (Setpoint + outlet disturbance) | 7.352 | | | 3.037 | | | 136.74 | | |
| Improvement: GA vs. manual tuning (%) | 13.00% | | | 11.38% | | | 16.84% | | |
| PSO (Setpoint + outlet disturbance) | Total IAE | | | Total ISE | | | Total ITAE | | |
| | 8.012 | | | 3.274 | | | 148.04 | | |
| Improvement: PSO vs. manual tuning (%) | 5.19% | | | 4.46% | | | 9.79% | | |

PSO improved respective IAE, ISE and ITAE with 5.19%, 4.46% and 9.79%, as compared with the three-element manual tuning. Moreover, the results reflect that the GA optimization in overall has more significantly improved the absolute error, large overshoot and consistency of control performance as compared with manual tunings.

F. Description of Curve Responses

Simulation analysis for servo and regulatory controls were performed with the same parameter settings, where the relative responses were compared. For the servo control, the water level was set between 1 – 3 meters in height. For regulatory controls, the feedwater inlet was set between 175

- 225 psi, whereas the steam outlet rate was set between 5000 – 7500 lbs/hr. The overall curve responses are shown in Fig. 6.

The graph depicts that the single loop tuning has resulted in significant overshoots and settling time. The curve response due to load swings of the feedwater inlet was improved by applying the cascade control algorithm. However, the cascade algorithm corresponds to the largest overshoots on the load swings of the steam outlet. To mitigate this issue, incorporating a feedforward algorithm to the control operations is essential and the improved control performance for disturbance steam outlet is shown by the

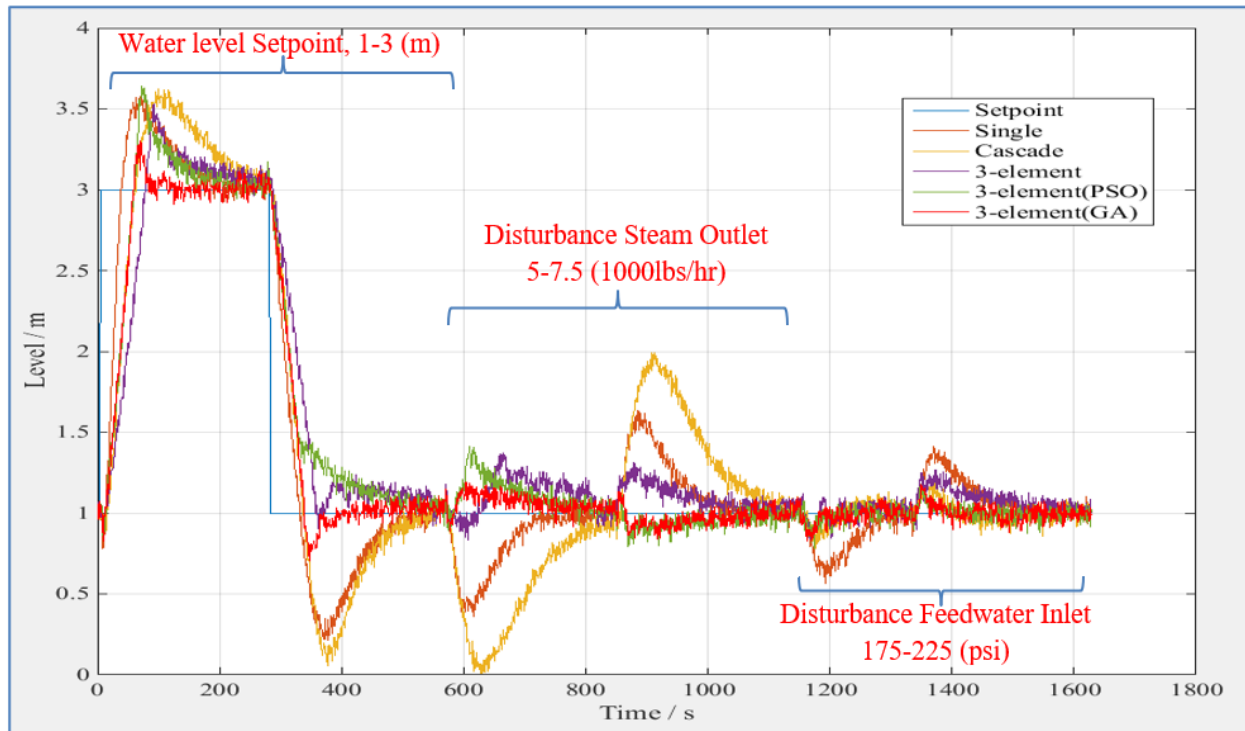


Figure 6. Curve Response of Single, Cascade and Three-element Loops

curve's response to the purple line. Besides, the multi-objective optimization analysis for the three-element loop was performed by using GA and PSO, respectively giving responses in green and red lines of Fig. 6. Both the GA and PSO produced the better curve responses particularly for disturbances on the steam outlet and feedwater inlet. Among both optimization analyses, GA provides PI controller settings to yield better curve responses, which means more controllable for servo and regulatory controls, as compared with PSO. Therefore, GA is more adaptable to the three-element control loop.

5. CONCLUSION

The research paper is essentially to denote that the applied optimization analysis has significantly improved the control performance for both servo and regulatory control objectives based on the findings of the case study. The analysis applied the boiler's water level function as the servo control, whereas the regulatory control has been imposed to the feedwater inlet and steam outlet function by changing the loads. The process and disturbance models of the Steam boiler drum function from the LOOP-PRO simulator have been used to calculate PI controller setting for manual tunings and optimization analysis. Manual tunings applied formulas to gain controller setting, whereas, optimization analysis to simulate an developed three-element based GUI toolbox for obtaining controller settings. For that, the determined UL and LL were applied.

In the integral error measurement, the multi-objective

optimization analysis obtained smaller error values as compared with manual tunings. In particular, GA shows higher controllability with the least integral errors among all the applied methods. On the other hand, the curve response shows that the tuning of three-element loop produced less overshoots and faster settling time as compared to the single and cascade loops. In particular, the simulation analysis also shows that the GA with Γ provided the fairest performance in reacting to the load swings of the steam outlet. Moreover, the research has successfully demonstrated the bound settings for the optimization analysis and determining the PI controller settings with Γ to enhance the effective control of three-element loop.

Nevertheless, the limitation of this research is lacked of physical facility to demonstrate optimization analysis to the real three-element process control. This research actually could be extended to real-time processes, whereby the MATLAB software is connected to the physical process and periodically performs the multi-objective optimization analysis while gaining process data from the physical processes. The recommended PID controller settings from the multi-objective optimization are to be instantly applied, in reacting to unexpected changes to the control loops.

REFERENCES

- [1] S. B. Joseph, E. G. Dada, A. Adidemi, D. O. Oyewola, and B. M. Khammas, "Metaheuristic algorithms for pid controller parameters tuning: review, approaches and open problems," *Heliyon*, pp. 1–29, 2020.



- [2] S. Nayak and S. Agashe, "Three element drum level control using matlab/simulink and opc," in *2nd International Conference for Convergence in Technology*, ser. Example Conference Proceedings. Mumbai, India: IEEE Explore, April 2017, pp. 607–609.
- [3] I. M. Chew, F. Wong, A. Bono, J. Nandong, and K. I. Wong, "Optimized computational analysis of feedforward and feedback control scheme using genetic algorithm techniques," in *11th Curtin University Technology, Science and Engineering (CUTSE) International Conference*, ser. 495. Miri, Malaysia: IOP Conf. Series: Materials Science and Engineering, December 2018, pp. 1–14.
- [4] N. V. Manh and V. T. Diep, "A synthesis method of robust cascade control system," *Journal of Automation and Control Engineering*, vol. 4(2), pp. 111–116, 2016.
- [5] R. Malhorta, N. Singh, and Y. Singh, "Genetic algorithms: Concepts, design for optimization of process controllers," *Canadian Center of Science and Education*, vol. 4(2), pp. 39–54, 2012.
- [6] A. Slowik, "Natural inspired methods and their industry applications – swarm intelligence algorithm," *IEEE Transactions On Industrial Informatic*, vol. 14(3), pp. 111–116, 2018.
- [7] P. Ouyang and V. Pano, "Comparative study of de, pso and ga for position domain pid controller tuning," *Algorithms*, vol. 8, pp. 697–711, 2015.
- [8] R. Trivedi and P. K. Padhy, "Fractional order automatic tuning of pi d controller for stable processes," *ISA Transactions*, vol. 99, pp. 351–360, 2020.
- [9] I. M. Chew, F. H. Juwono, and W. K. Wong, "Ga-based optimization for multivariable level control system: A case study of multi-tank system," *Engineering Journal*, vol. 26, no. 5, pp. 25–41, 2022.
- [10] I. M. Chew, F. Wong, J. Nandong, and K. I. Wong, "Genetic algorithm optimization analysis for temperature control system using cascade control loop model," *International Journal of Computing and Digital Systems*, vol. 9(1), pp. 119–127, 2020.
- [11] R. Zhou, C. Hu, and Y. Zhu, "Comparative study of performance-oriented feedforward compensation strategies for precision mechatronic motion systems," *IEEE Access*, vol. 10, pp. 100 812–100 823, 2022.
- [12] Q. Jin, Z. Yin, and Q. Dai, "Numerical and experimental study of feedforward and feedback control for microchannel cooling system," *International Journal of Thermal Sciences*, vol. 179, p. 107643, 2022.
- [13] N. Ahooghalandari, R. Shadi, and A. Fakharian, " \mathcal{H}_∞ robust control design for three-element industrial boiler supervisory system," in *2022 8th International Conference on Control, Instrumentation and Automation (ICCIA)*. Tehran, Iran Islamic Republic of: IEEE, March 2022, pp. 1–6.
- [14] B. Shi, R. Shi, and F. Wang, "Design of an adaptive feedforward/feedback combined control for piezoelectric actuated micro positioning stage," *Precision Engineering*, vol. 78, pp. 199–205, 2022.
- [15] P. Quintanilla, D. Navia, F. Moreno, S. Neethling, and P. Brito-Parada, "A methodology to implement a closed-loop feedback-feedforward level control in a laboratory-scale flotation bank using peristaltic pumps," *MethodsX*, vol. 10, pp. 1–15, 2023.
- [16] I. Kaya and M. Nalbantoğlu, "Simultaneous tuning of cascaded controller design using genetic algorithm," *Electrical Engineering*, vol. 98, pp. 299–305, 2016.
- [17] M. Ali, S. T. Zahra, K. Jalal, A. Saddiqa, and M. F. Hayat, "Design of optimal linear quadratic gaussian (lqg) controller for load frequency control (lfc) using genetic algorithm (g.a) in power system," *International Journal of Engineering Works*, vol. 5, pp. 40–49, 2018.
- [18] H. Elgothamy, H. S. Abdel-Aty-Zohdy, M. A. Zohdy, and M. Hua, "Application of enhanced genetic algorithm to symbolic audubon data," *International Journal of Engineering Works*, vol. 7, pp. 55–59, 2018.
- [19] K. Vijayan, P. Ranjithkumar, and B. Shanmugarajan, "Comparison of response surface methodology and genetic algorithm in parameter optimization of laser welding process," *Applied Mathematics Information Sciences*, vol. 12, pp. 239–248, 2018.
- [20] S. Dawood, A. K. Mahmood, and M. A. Ibrahim, "Comparison of pid, ga and fuzzy logic controllers for cruise control system," *International Journal of Computing and Digital Systems*, vol. 5, pp. 311–319, 2018.
- [21] U. Khair, A. Perdana, A. Budiman, Y. D. Lestari, and D. Hidayat, "Genetic algorithm modification analysis of mutation operators in max one problem," in *2018 Third International Conference on Informatics and Computing (ICIC)*. Palembang, Indonesia: IEEE Xplore, March 2023, pp. 1–6.
- [22] W. Q. Wang, M. J. Li, J. Q. Guo, and W. Q. Tao, "A feedforward-feedback control strategy based on artificial neural network for solar receivers," *Applied Thermal Engineering*, vol. 224, pp. 1–11, 2023.
- [23] A. A. A. Esmine and G. Lambert-Torres, "Application of particle swarm optimization to optimal power systems," *International Journal of Innovative Computing, Information and Control (IJICIC)*, vol. 8(3A), pp. 1705–1716, 2012.
- [24] J. W. Lian and H. Y. Chen, "Feedforward and feedback control for piezoelectric-actuated systems using inverse prandtl-ishlinskii model and particle swarm optimization," in *International Conference on Advanced Mechatronic Systems*. Kumamoto, Japan: IEEE Xplore, August 2014, pp. 313–318.
- [25] M. Sayed, G. S. M., and H. A. Kamal, "Gain tuning pi controllers for boiler turbine unit using a new hybrid jump pso," *Journal of Electrical Systems and Information Technology*, vol. 2, pp. 99–110, 2015.
- [26] T. Gao, J. Li, S. Zhu, X. Yang, and H. Zhao, "H optimization of three-element-type dynamic vibration absorber with inerter and negative stiffness based on the particle swarm algorithm," *Entropy*, vol. 25, pp. 1–25, 2023.
- [27] M. Rafiei and G. R. Ansarifard, "Space nuclear reactor fuel design based on dynamic analysis and ga pso optimization," *Progress in Nuclear Energy*, vol. 143, p. 104043, 2022.
- [28] I. M. Chew, W. K. Wong, and J. Nandong, "Optimization analysis of nonlinear process using genetic algorithm," *Journal of Information Science and Engineering*, vol. 36, pp. 909–921, 2022.



Chew Ing Ming received the Bachelor of Engineering degree in electrical engineering (major in instrumentation and control) from the University Tun Hussein Onn, Batu Pahat, Johor, Malaysia, in 2002 and the Ph.D. degree in electrical and electronics engineering from University Malaysia Sabah, Sabah, Malaysia, in 2020. He is currently a lecturer at Curtin University Malaysia in Miri, Sarawak, Malaysia. Since 2020, he

served as the program coordinator for the Bachelor of Electrical and Electronics Engineering, Electrical and Computer Department from Curtin University Malaysia. His research interest includes optimization, PID Control and embedded systems IoT



Filbert H. Juwono received his B.Eng degree in electrical engineering and M.Eng degree in telecommunication engineering from the University of Indonesia, Depok, Indonesia in 2007 and 2009, respectively. He gained Ph.D. degree in electrical and electronic engineering from The University of Western Australia, Perth, WA, Australia in 2017. He is currently an Assistant Professor at Xi'an Jiaotong - Liverpool University. His

research interests include signal processing for communication, power-line communications, machine learning applications, and biomedical engineering. Currently, he serves as an Associate Editor for IEEE Access, a Review Editor for Frontiers in Signal Processing, and an Editor-in-Chief for Green Intelligent Systems and Applications journal.



Wong Wei Kitt received the M.Eng. and Ph.D. degrees from Universiti Malaysia Sabah in 2012 and 2016, respectively in Computer Engineering. Before joining academia, he was with the telecommunication and building services industry. He is currently serving as an Associate Professor with the Department of Electrical and Computer Engineering, Curtin University Malaysia. His research interests include

embedded system development, machine learning applications, and image processing.